Pol. J. Environ. Stud. Vol. 30, No. 1 (2021), 273-282
DOI: *10.15244/pjoes/120156* ONLINE PUBLICATION DATE: 2020-07-31

Original Research

Enhancing Photocatalytic Degradation of Methylene Blue Using ZnO/Carbon Dots Nanocomposite Derived From Coffee Grounds

Akhiruddin Maddu*, Reny Meliafatmah, Erus Rustami

Department of Physics, Bogor Agricultural University (IPB University),
Jl. Meranti, Gedung Wing S, Kampus IPB Dramaga, Bogor 16680, Indonesia

Received: 9 December 2019
Accepted: 6 April 2020

Abstract

In this article, we report the enhancement of the photocatalytic activity of ZnO/carbon dots (CDs) nanocomposite in degrading methylene blue (MB) dye. Carbon dots (CDs) were synthesized by a hydrothermal method utilizing coffee grounds as a carbon source. ZnO/CDs nanocomposite was synthesized by a single-step and *in-situ* sonochemical process. The particle size of CDs measured by dynamic light scattering (DLS) was found at about 7.7 nm. The result of X-ray diffraction analysis confirmed that the hexagonal wurtzite structure of ZnO nanoparticle has a small crystal size and the lattice parameters decreasing due to CDs addition. The surface morphology images were taken by scanning electron microscopy (SEM) shows a very fine particle both for pure ZnO nanoparticle and ZnO/CDs nanocomposite. The result of Energy Dispersive X-Ray Spectroscopy (EDXS) analysis confirmed the presence of the carbon element in the ZnO/CDs nanocomposite indicated that the nanocomposite has been formed. The result of the photocatalytic test showed that the ZnO/CDs nanocomposite photocatalyst had significantly increased photocatalytic activity compared to the pure ZnO nanoparticle photocatalyst. ZnO/CDs nanocomposite photocatalyst resulted in a photodegradation rate three times higher than pure ZnO nanoparticle photocatalyst and nine times higher than the photolysis treatment (without photocatalyst). Whereas the degradation efficiency of MB using ZnO/CDs nanocomposite photocatalyst was twice higher than using pure ZnO nanoparticles and four times higher than photolysis treatment.

Keywords: carbon dots, coffee grounds, nanocomposite, photocatalysis, ZnO nanoparticle

Introduction

Fujishima and Honda discovered a water splitting phenomenon in their experiment on the electrochemical photolysis of water used semiconductor electrode [1]. During their experiment, Fujishima and Honda discovered a photocatalytic activity of TiO_2 and began testing this semiconductor as a photocatalyst. Since then the development of the photocatalysis mechanism involving the semiconductor material as a photocatalyst to decompose the organic dyes began to increase very

*e-mail: akhiruddin@apps.ipb.ac.id

rapidly until now. The photocatalysis process takes place through the activation of semiconductor materials by suitable photon energy that generates the active charges (electron-hole pairs) which will induce catalytic reactions at semiconductor surfaces [2-5]. Traditionally, the TiO_2 is a metal-oxide-semiconductor that is the earliest and most commonly used as a photocatalyst to decompose organic dyes [4-8].

As a consequence of early Fujishima and Honda's experiment, there are further numerous experiments on the use of semiconductors, such as ZnO, as photocatalysts for the decomposition of some organic pollutants [9-14], but the photocatalytic activity of ZnO is no better than TiO_2. Hence, various attempts have been conducted to enhance the photocatalytic activity of ZnO by various modifications such as doping or hybridization or compositing with other materials. This modification changes the optical absorption property of photocatalyst while making charges transfer more effective in the photocatalysis mechanism. Some previous studies have modified ZnO photocatalyst by doping with various elements such as silver [15], magnesium [16], iron [17, 18], carbon [18], and nitrogen [19-21]. Other efforts have making heterostructures or heterojunctions of ZnO with other semiconductor materials such as SnO_2 [22], ZnS [23], NiO [24], CdS [25], and CdO [26]. In addition, several studies have conducted a hybridization of ZnO with g-C_3N_4 to enhance its photocatalytic activity [27-29]. Previous studies have also conducted modification of ZnO with carbon nanomaterials to form heterostructures including carbon nanotube [30], carbon nanofiber [31], activated carbon fiber [32], and carbon dots [33-36].

Carbon dots (CDs) have been developed as new photocatalyst materials because of their ability to generate charge carriers when is exposed with appropriate photon energy. As a nanomaterial, CDs are known to be able to absorb the wide spectrum of the electromagnetic energy from UV to visible spectrum (blue-green region), so that they can contribute to the photocatalysis mechanism, both alone or in combination with various semiconductor materials [37-40]. CDs have been combined with several semiconductor materials to form nanocomposites or heterostructures, such as with ZnO, to enhance charges transfer in the photocatalyst [33-36].

This study aims to enhance the photocatalytic activity of ZnO nanoparticles by the addition of CDs derived from coffee grounds which is the rest of steeping which is thrown away after being drunk by coffee drinkers. This addition is aimed to facilitate the transfer of photon-generated charges (electron-hole pairs) by preventing early recombination in bulk ZnO photocatalyst. The CDs addition into ZnO nanoparticles can accelerate the photocatalytic reaction which in turn would increase photocatalytic activity and enhance the degradation efficiency and degradation rate of the dye. Synthesis of CDs was conducted by a hydrothermal method utilizing coffee grounds as carbon source, then the synthesis of ZnO/CDs nanocomposite was carried out in one-step and one-pot process by the sonochemical method.

Materials and Methods

Synthesis and Characterization of Carbon Dots (CDs)

To synthesis carbon dots (CDs), 2.5 g of coffee grounds was poured into 250 mL of NaOH (0.2 M) solution while stirred until fully mixed. The mixture was poured into a stainless steel autoclave to be hydrothermally processed at 100ºC for 1 hour. The dark brown suspension resulted was filtered to separate the precipitate from the supernatant. The supernatant containing carbon nanoparticles (CDs) was diluted with distilled water then optically characterized to determine their optical absorption by using UV-Vis spectrophotometer (USB4000 Ocean Optics Spectrophotometer). The particle size distribution of CDs was measured by dynamic light scattering (DLS) method using Particle Size Analyzer (PSA, VASCO).

Synthesis and Characterization of Photocatalysts

Synthesis of pure ZnO nanoparticle photocatalyst was conducted by dissolving 4 g of $Zn(CH_3COO)_2.2H_2O$ (0.25 M) in 100 mL NaOH (0.2 M) solution. The mixed solution was transferred into the beaker glass (150 mL) then placed into the ultrasonic bath which has been filled with enough water. Ultrasonic bath is turned on for 2 hours for sonochemical processing. The resulting precipitate was filtered and then dried on the hotplate at 100 °C for 2 hours. The dry precipitate powder was annealed in the furnace at 300ºC for 5 hours to obtain pure ZnO nanoparticle powder.

Synthesis of ZnO/CDs nanocomposite photocatalyst was conducted by *in-situ* sonochemical method in one-step and one-pot using an ultrasonic bath. As much as 4 g of $Zn(CH_3COO)_2.2H_2O$ was dissolved in 100 mL of CDs solution that has been derived from coffee grounds. The pH 12 of the mixed solution was adjusted by gradually dropping of NaOH (8 M) solution while stirred. Then the mixed solution was transferred into the beaker glass (150 mL) then placed in the ultrasonic bath which has been filled with enough water. Ultrasonic bath is turned on for 2 hours for sonochemical processing. The resulting suspension was centrifuged at 3000 rpm for 30 min to obtain a brown precipitate. The resulting precipitate was filtered and washed by distilled water three times alternately to remove impurities then dried on the hotplate at 100ºC for 2 hours. The dry brown powder was annealed in the furnace at 300ºC for 5 hours to obtain brown ZnO/CDs nanocomposite.

Both pure ZnO nanoparticle and ZnO/CDs nanocomposite were characterized by using X-ray diffraction (XRD) to determine their crystal parameters

including crystal phase, crystal lattices, and crystallite size. Morphology of the products was investigated by using scanning electron microscopy (SEM) and chemical composition was determined by using Energy Dispersive X-ray Spectroscopy (EDXS) analysis taken simultaneously with SEM images capturing.

Photodegradation Testing of Methylene Blue

Photodegradation treatments of metylene blue (MB) dye were conducted, namely UV photolysis, photocatalysis treatment using pure ZnO nanoparticle, and photocatalysis treatment using ZnO/CDs nanocomposite as photocatalyst. Photocatalysis treatment was conducted by directly exposing the UV light to the MB dye solution without photocatalyst. Photocatalysis treatments was carried out in a cuvette under UV light irradiation using a 6W UVB lamp (360 nm). As much as 4 mL of MB dye solution with an initial concentration of 5 ppm was poured into the cuvette. Then, 1 mg of each photocatalyst (pure ZnO nanoparticle and ZnO/CDs nanocomposite) was dispersed into the MB solution. Before irradiation, the solution was stirred to achieve the adsorption-desorption equilibrium between MB dye and photocatalysts. Furthermore, the dye-photocatalyst suspension was irradiated by UV light at room temperature for 150 minutes. Every 30 minutes of irradiation, the cuvette is inserted into the cuvette holder of UV-Vis spectrophotometer (USB4000 Ocean Optics Spectrophotometer) to be measured the absorption spectra of the MB solution after irradiation. The absorbance spectra were used to determine the concentration of MB solution after every 30 minutes of irradiation for each solution. The concentration of MB solution is determined based on the absorbance change at the specific absorption wavelength of the MB solution. By using a standard curve of MB, the quantitative concentration of MB can be determined for each photodegradation treatment. Photodegradation efficiency (η) is calculated based on the absorbance of MB dye at the specific absorption wavelength by the equation as follows:

$$\eta(\%) = (A_o - A_t)/A_o \times 100\% \quad (1)$$

...where A_o is the initial absorption of the dye, and A_t is the absorption of the dye at a given UV irradiation time.

To determine the photodegradation rate (rate constant) of MB dye, we have to make a linear curve between Ln (C/C_o) and irradiation time (t) according to equation (2), namely the natural logarithmic relationship between the concentration of MB and the irradiation time (t) as relation below [35]

$$\ln (C/C_o) = -kt \quad (2)$$

...where C_o is the concentration of MB solution at t = 0, i.e the concentration before treatment, C is the concentration of MB every treatment time t (second), and *k* is a rate constant of MB degradation.

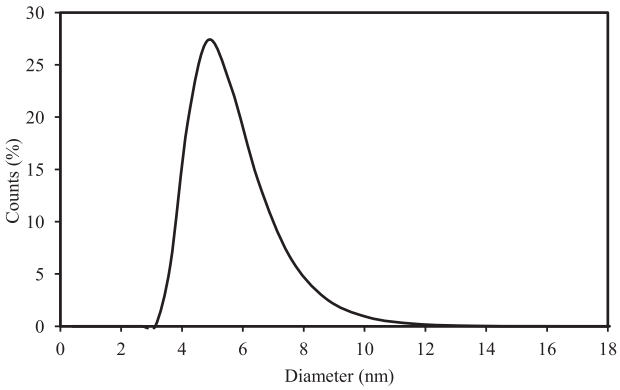

Fig. 1. The particle size distribution of carbon dots (CDs).

Results and Discussion

Characteristics of Carbon Dots (CDs)

The particle size distribution of CDs was measured by using particle size analyzer (PSA) based on dynamic light scattering (DLS). Fig. 1 shows the particle size distribution of CDs derived from coffee grounds. The resulting curve is wide enough indicating that the particle size of CDs varies greatly, from around 3 to 10 nm, with a predominance of particle size at around 7.74 nm. These results indicate that the carbon nanoparticle that has been derived from coffee grounds by hydrothermal method has nanostructure with a very small size so that it can be stated as quantum dots. Fig. 2 shows the absorption spectrum of the CDs solution covering quite broad of the electromagnetic spectrum from UV (~ 350 nm) to the visible (~ 600 nm) range with an absorption peak at around 410 nm (violet). Based on this characteristic, CDs can be involved in photocatalysis mechanisms because of the ability to absorb UV-visible energy of electromagnetic spectrum

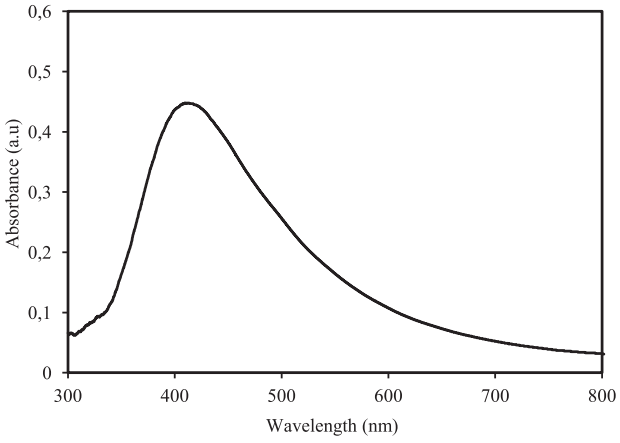

Fig. 2. Absorption spectra of carbon dots (CDs).

which can generate more electron-holes pairs to induce photocatalysis reaction, as a result, can improve the photocatalytic activity of CDs/ZnO heterostructure [33-36].

Crystal Parameters of Photocatalysts

Both pure ZnO nanoparticle and ZnO/CDs nanocomposite were characterized by using X-ray diffraction to investigate their crystal phase, crystal lattice, and crystallite size. Fig. 3 shows a diffraction pattern of both samples. There is no significant difference in both diffraction patterns where the diffraction peaks were identified as belonging to ZnO. There is no carbon phase (C) present in a diffraction pattern for both samples, including in ZnO/CDs nanocomposite sample. This is because the fraction of CDs in the ZnO/CDs nanocomposite sample is relatively small when compared to the fraction of ZnO nanoparticle.

Diffraction pattern of pure ZnO nanoparticle, as in Fig. 3a), shows the ZnO diffraction peaks respectively present at 2θ = 31.76º, 34.41º, 36.24º, 47.53º, 56.59º, 62.82º, 67.92º which corresponding to the lattice planes (hkl) of (100), (002), (101), (102), (110), (103), and (112). All the peaks present after annealing the precursor at 300ºC are assigned as hexagonal wurtzite structure of ZnO (JCPDS card No. 36-1451) [15-21]. While, the diffraction pattern for ZnO/CDs nanocomposite, as in Fig. 3b), almost no difference when compared to the diffraction pattern of pure ZnO nanoparticle sample. Therefore, the addition of CDs into ZnO nanoparticles almost not change the crystal phase of ZnO.

The crystal phase of ZnO nanoparticle can be confirmed based on its lattice parameters. The lattice parameter values were calculated using the Cohen method based on the diffraction pattern of sample. The calculation results show that the lattice parameter values obtained correspond to the hexagonal wurtzite structure of ZnO (JCPDS card No. 36-1451) [15-21]. The results of the lattice parameter calculation are presented in Table 1. Data obtained show a small

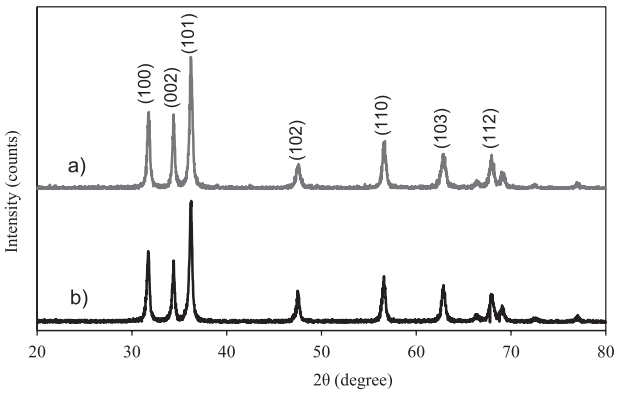

Fig. 3. XRD pattern of a) pure ZnO nanoparticle and b) ZnO/CDs nanocomposite.

Table 1. Lattice parameters of pure ZnO nanoparticle and ZnO/CDs nanocomposite.

Sample	Lattice parameters [Å]		Accuracy [%]	
	a	c	a	c
ZnO	3.2503	5.2089	99.96	99.93
ZnO/CDs	3.2463	5.1986	99.91	99.88

variation in the lattice spacing of ZnO nanoparticle due to CDs addition. The lattice spacing for the pure ZnO nanoparticle is a = b = 3.2503 Å and c = 5.2089 Å. While for ZnO/CDs nanocomposite, the lattice spacing is a = b= 3.2463 Å c = 5.1986 Å, there is a slightly decreased when compared to pure ZnO nanoparticle. Decreasing the value of lattice spacing due to carbon insertion into the lattice structure of ZnO nanoparticle. The accuracy of the calculating results of lattice parameters is smaller for ZnO/CDs nanocomposite than pure ZnO nanoparticle (Table 1), this is because of the decrease in lattice spacing due to the addition of CDs.

The average crystallite size (ACS) of the samples was calculated based on full width at half maximum (FWHM) of diffraction pattern using the Debye-Scherrer equation (3) as follows:

$$D = k\lambda/\beta \cos\theta \quad (3)$$

...where D is the crystal size, k is Scherrer constant (0.89), λ is X-ray wavelength (0.154 nm), β is the peak full width at half maximum (FWHM), and θ is the Bragg diffraction angle.

Fig. 3 shows a considerable peak widening in the diffraction pattern of ZnO nanoparticle indicating the FWHM value is relatively large. Data presented in Table 2 shows the FWHM of pure ZnO nanoparticle slightly larger than ZnO/CDs nanocomposite that indicating that the average crystallite size of pure ZnO nanoparticle smaller than ZnO/CDs nanocomposite. The calculation results of the ACS of both samples are presented in Table 2. It shows that the addition of CDs greatly affected the ACS of ZnO/CDs nanocomposite. The ACS of ZnO/CDs nanocomposite larger than pure ZnO nanoparticle. These results demonstrate that CDs were successfully incorporated into ZnO lattice. The addition of CDs resulted in extending the distance between the atoms in the crystal lattice of ZnO so that the crystallite size increased.

Table 2. The average crystallite size (ACS) of pure ZnO nanoparticle and ZnO/CDs nanocomposite.

Sample	FWHM (101)	The average crystallite size [nm]
ZnO	0.344	30.622
ZnO/CDs	0.307	34.694

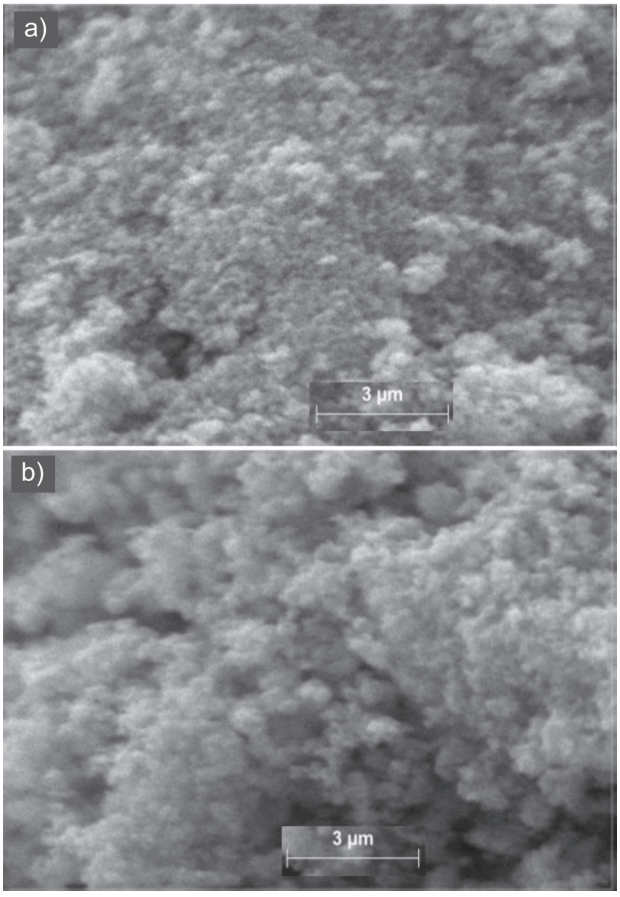

Fig. 4. SEM images of a) pure ZnO nanoparticle and b) ZnO/CDs nanocomposite.

Morphology and Chemical Composition of Photocatalysts

Surface morphology images of both photocatalyst samples were taken by using scanning electron microscopy (SEM). Fig. 4 shows morphology images of the pure ZnO nanoparticle and ZnO/CDs nanocomposite with a magnification of 10,000 times. Both images show a homogeneous surface morphology with very fine granules. Morphology of pure ZnO nanoparticle appeared finer than ZnO/CDs nanocomposite which appeared to clot. It was seen that the size of the granules for the pure ZnO nanoparticle was smaller than the ZnO/CDs nanocomposite. This is because, in the ZnO/CDs nanocomposite, ZnO particles are covered by CDs, so slightly increasing the size of the ZnO particles.

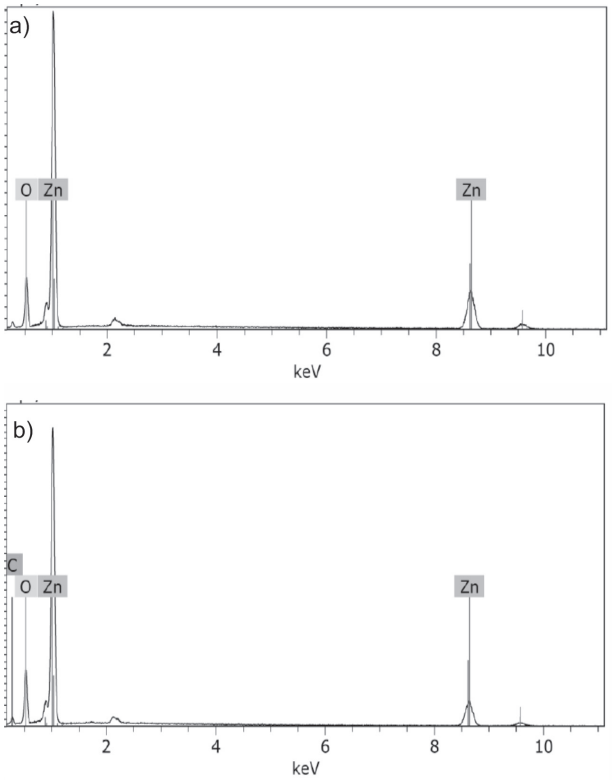

Fig. 5. EDXS spectra of a) pure ZnO nanoparticle and b) ZnO/CDs nanocomposite.

The chemical composition of the photocatalyst materials was identified based on data from Energy-Dispersive X-ray spectroscopy (EDXS). Fig. 5 shows the EDXS spectra for both pure ZnO nanoparticle and ZnO/CDs nanocomposite. Peaks of zinc and oxygen elements present in the spectra where the peak of zinc dominating the spectra. Spectra of ZnO/CDs nanocomposite shows a peak of carbon indicating the presence of carbon elements originating from CDs in the nanocomposite. Table 3 presents the elemental composition of both photocatalyst materials. The percentage ratio of Zn and O for the pure ZnO nanoparticle is more than 1, which is 1.32, indicating that in the sample, not all Zn atoms bond to the O atom but there are several Zn atoms stand-alone. The sample of ZnO/CDs nanocomposite has the percentage ratio of Zn and O is 0.77 and is worth 1.29 for the percentage ratio of Zn and C, this indicates that Zn atoms are more bound to C than O formed at CDs.

Table 3. EDXS analysis of pure ZnO nanoparticles and ZnO/CDs nanocomposite.

Sample	Element			Ratio	
	C (at. %)	O (at. %)	Zn (at. %)	Zn/O	Zn/C
ZnO	-	43.18	56.82	1.32	-
ZnO/CDs	24.92	42.52	32.57	0.77	1.29

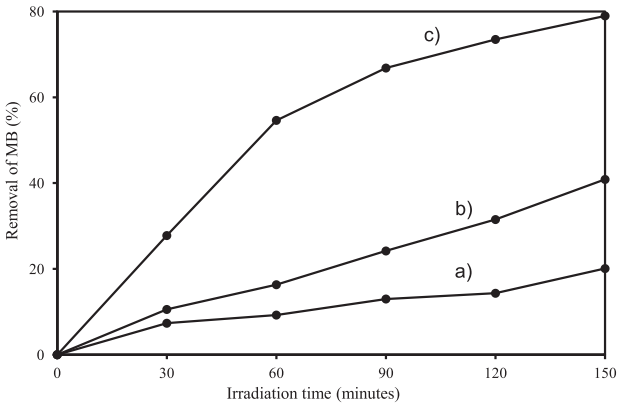

Fig. 6. Removal percentage of MB dye: a) photolysis, b) photocatalysis using pure ZnO nanoparticle, and c) photocatalysis using ZnO/CDs nanocomposite.

Photocatalytic Activity of Photocatalysts

Three different photodegradation treatments of MB dye were conducted, namely UV photolysis (without photocatalyst), photocatalysis with pure ZnO nanoparticle, and photocatalysis with ZnO/CDs nanocomposite. Photodegradation treatments were conducted using a 6W UVB (360 nm) lamp as a light source. As a control treatment, photolysis was conducted by directly exposing the UV source to MB solution without photocatalyst contains. Photocatalytic degradation of MB dye was conducted by exposing the UV light to the MB-photocatalyst suspension for both photocatalysts used, which is pure ZnO nanoparticle and ZnO/CDs nanocomposite. UV Lamp used as light source because the ZnO photocatalyst has strong absorption in the UV spectrum and CDs also has UV absorption.

Fig. 6 shows the percentage of dye removal over time for the three photodegradation treatments for 150 minutes. Photolysis treatment did not result in a significant decrease of MB dye, it only able to degrade 20% of MB compounds during 150 minutes of UV irradiation, this is because the UV energy is not able to break quickly and optimally chemical bonds in the MB compound. The photocatalysis treatment was significant in removing MB dye in solution, especially those using ZnO/CDs nanocomposite photocatalyst. The use of pure ZnO nanoparticle was only able to reduce 40% of MB content in solution while the use of ZnO/CDs nanocomposite photocatalyst was able to reduce nearly 80% of MB content during 150 minutes of photocatalysis treatment. Therefore, the degradation of MB dye for photocatalytic treatment using ZnO/CDs nanocomposite as photocatalyst much faster than using pure ZnO nanoparticle.

Fig. 7 shows the curves of the Ln (C/Co) versus time (t) for the three different photodegradation treatments. The slope of the curve represents the photodegradation rate (rate constant) of the MB dye, the higher the slope of the photodegradation curve the higher the photodegradation rate. The photocatalytic treatment using ZnO/CDs nanocomposite photocatalyst shows a very large slope when compared to the curves for photocatalytic treatment using pure ZnO nanoparticle as well as by photolysis treatment. The rate constants of the photodegradation treatments are shown in Table 4, it is found that photocatalysis treatment using ZnO/CDs nanocomposite as photocatalyst three times more effective than photocatalysis treatment using pure ZnO nanoparticle, even almost eight times more effective than photolysis treatment (directly irradiation by UV lamp). The addition of CDs greatly contributed to the increase in the photocatalytic activity

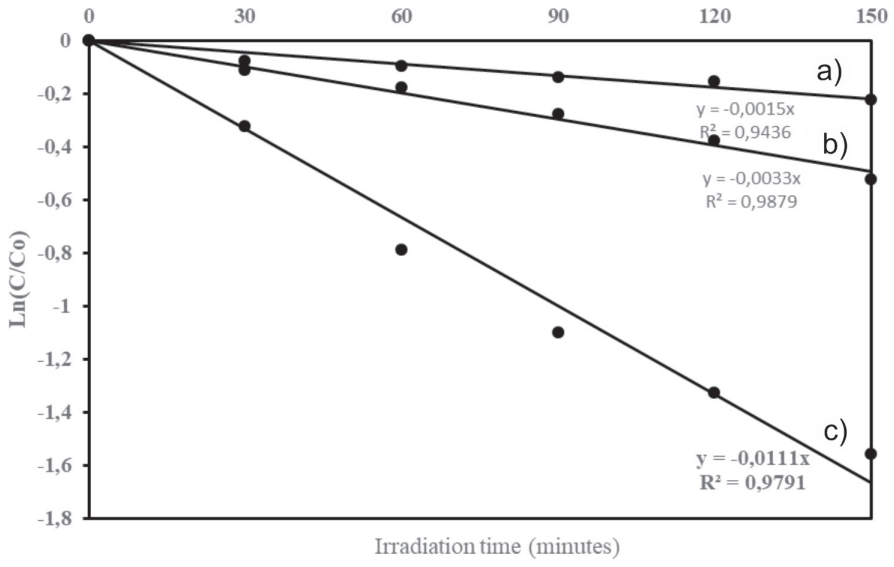

Fig. 7. Degradation rates of MB dye: a) photolysis, b) photocatalysis using pure ZnO nanoparticle, and c) photocatalysis using ZnO/CDs nanocomposite

Table 4. The photodegradation parameters of the MB dye by different treatments.

Treatment	Photodegradation rate [min^{-1}]	Photodegradation efficiency [%]
Photolysis	0.0015	20.97
Photocatalysis with ZnO	0.0033	41.54
Photocatalysis with ZnO/CDs	0.0111	80.34

of ZnO/CDs nanocomposite in degrading MB dye compound.

The degradation efficiency of three photodegradation treatments is presented in Table 4. It is found that the photodegradation efficiency for photocatalysis treatment using ZnO/CDs nanocomposite is almost twice higher than using pure ZnO nanoparticles, and four times higher than photolysis treatment. Photocatalytic degradation using ZnO/CDs nanocomposite able to degrade the MB content in solution up to 80% for 150 minutes irradiation by UV light. The obtained result in this study is comparable to those resulted by Yu et al which using ZnO/CDs nanocomposites as photocatalysts, which are able to degrade 80% of benzene [36]. However, there was a difference, Yu et al achieved 80% degradation after photocatalysis treatment for 4 hours whereas in this study only about 150 minutes irradiation by UV light. Yu et al used three 8 W visible light lamps to irradiate the photocatalyst. This result also comparable with the result obtained by Bozetine et al which also using ZnO-CDs nanocomposite as a photocatalyst to degrade the rhodamine B dye [35]. However, Bozetine et al. found a photodegradation rate higher than this study an also faster to achieve 90% degradation of RhB. Bozetine used visible light to irradiate the photocatalyst.

Enhanced photocatalytic activity of ZnO/CDs nanocomposite is due to the charges (electron-hole pairs) transfer mechanism at the photocatalyst surface more effective. The heterojunction formed in ZnO/CDs nanocomposite increases the separation of photogenerated electron-hole pairs so that the transfer mechanism of the electron-hole pairs becomes more effective which in turn enhanced the photocatalytic activity of the photocatalyst. Rapid separation of electron-hole pairs avoids early recombination in the bulk of photocatalyst. It is known that one of the constraints that result in a low photocatalytic activity is the early recombination mechanism in the bulk of the photocatalyst. Therefore, modifications are needed to facilitate the transfer of active charges to the photocatalyst surface before early recombination occurs within the bulk of ZnO. The obtained result confirmed that the ZnO/CDs heterostructure successfully facilitated the transfer process of electron-hole pairs between the ZnO and CDs which induce the photocatalytic reaction at the surface of the photocatalyst to enhance the degradation of the MB dye.

Fig. 8 illustrates the energy diagram of the heterostructure of ZnO/CDs nanocomposite. The position of the lowest unoccupied molecular orbital (LUMO) and the highest occupied molecular orbital (HOMO) of both materials determines the transfer mechanism of active charges (electron-hole pairs) that photogenerated, as well as affect the reactions that occur on the surface of the photocatalyst. The position of the LUMO and HOMO energy levels of CDs are -3.99 eV and -7.04 eV [41], while the conduction band (CB) and valence band (VB) of ZnO are -4.05 eV and -7.25 V [42]. Therefore, the HOMO energy level of CDs higher than the conduction band of ZnO, likewise, the HOMO energy level of CDs is also higher than the valence band of ZnO [33, 42]. Electrons photogenerated in the LUMO of CDs are rapidly injected into the conduction band of ZnO, while holes generated in the valence band of ZnO are easily injected into the HOMO energy level of CDs. These two active charges together increase the photocatalytic reaction on the surface of photocatalysts.

Oxidative reactions occur simultaneously at both the LUMO of CDs and conduction band (CB) of ZnO, as well as the reductive reactions also occur simultaneously at the HOMO of CDs and valence band

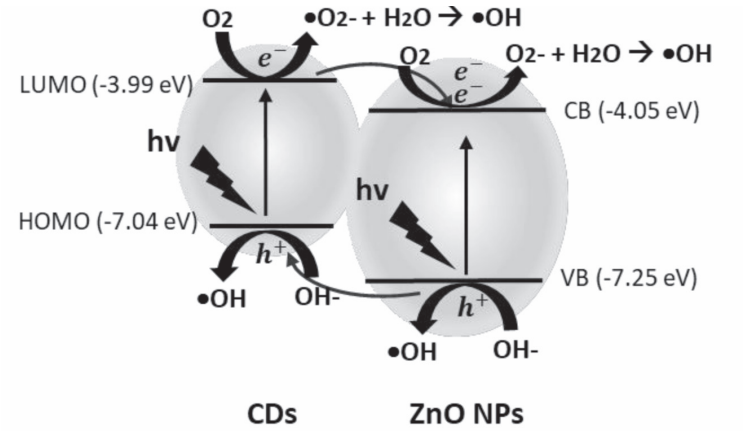

Fig. 8. Photocatalysis mechanism scheme of ZnO/CDs nanocomposite.

(VB) of ZnO. Both oxidative and reductive reactions generate free radicals (e.g. hydroxyl radicals: •OH) that very oxidative in nature and able to undergo secondary reactions that can decompose organic compounds like dyes. The simultaneous oxidative and reductive reactions on the photocatalyst surface will increase the formation of free radicals (•OH) thus enhancing the photocatalytic activity of the ZnO/CDs nanocomposite system.

On the other hand, the photogeneration of the electron-hole pairs depends on the bandgap energy of materials. The bandgap energy of ZnO is 3.20 eV [33, 42], while the bandgap energy of CDs is 3.05 eV [41]. Therefore, CDs tend to absorb from the UVB to the blue region while ZnO fully absorbs the UV region of the electromagnetic spectrum. The combination of ZnO and CDs widen the absorption spectrum of the nanocomposite thereby increasing the number of active charges (electron-hole pairs) that can be generated by light photon (photogeneration). Photogeneration of active charges occurs simultaneously in both materials through exposure to UV light used. The amount of charge which is photogenerated influence the probability of a photocatalytic reaction occurring on the surface of the photocatalysts.

Conclusions

CDs have been successfully synthesized from coffee grounds by hydrothermal method with an average particle size of 7.74 nm. The combination of CDs and ZnO nanoparticles that forming a nanocomposite system barely changes the crystal phase but increased the average crystal size of the ZnO nanoparticles, also significantly changes the morphology of ZnO nanoparticles. The combination of CDs and ZnO nanoparticles form a heterostructure to facilitate the transfer mechanism of photogenerated electrons-holes pairs that induce oxidative-reductive reactions at the surface of photocatalysts. The photocatalytic activity of ZnO/CDs nanocomposite significantly increased in degrading MB dye. The photodegradation rate of MB dye increased almost three times when utilizing ZnO/CDs nanocomposite photocatalyst compared to pure ZnO nanoparticle as a photocatalyst, even almost nine times higher than photolysis treatment. The enhanced photocatalytic activity of ZnO/CDs nanocomposite due to the transfer mechanism of electron-hole pairs more effective and efficient in accelerating free radicals production (e.g. hydroxyl radicals) on the surface of the photocatalysts.

Acknowledgements

This study was fully supported by the Department of Physics, Bogor Agricultural University, Bogor, Indonesia. The authors thank the Department of Physics for any support, especially for using any facilities in completing this study.

Conflict of Interest

The authors declare no conflict of interest.

References

1. FUJISHIMA A., HONDA K. Electrochemical Photolysis of Water at a Semiconductor Electrode. Nature, **238**, 37, **1972**.
2. NAKATA A., FUJISHIMA A. TiO_2 photocatalysis: Design and applications. Journal of Photochemistry and Photobiology C: Photochemistry Reviews, **13**, 169, **2012**.
3. SCHNEIDER J., MATSUOKA M., TAKEUCHI M., ZHANG J., HORIUCHI Y., ANPO M., BAHNEMANN D.W. Understanding TiO_2 Photocatalysis: Mechanisms and Materials. Chemical Review, **114**, 9919, **2014**.
4. NAKATA K., OCHIAI T., MURAKAMI T., FUJISHIMA A., Photoenergy conversion with TiO_2 photocatalysis: New materials and recent applications. Electrochimica Acta, **84**, 103, **2012**.
5. YUANGPHO N., TRINH D.T.T., CHANNEI D., KHANITCHAIDECHA W., NAKARUK A. The influence of experimental conditions on photocatalytic degradation of methylene blue using titanium dioxide particle. Journal of the Australian Ceramic Society, **54**, 557, **2018**
6. MADDU A., DENI I., SOFIAN I. Effect of Cu doping on structural properties and photocatalytic activity of TiO_2 nanoparticles synthesized by sol-gel method. Journal of Ceramic Processing Research, **19** (1), 25, **2018**.
7. WU W., ZHANG L., ZHAI X., LIANG C., YU K. Preparation and photocatalytic activity analysis of nanometer TiO_2 modified by surfactant. Nanomaterials and Nanotechnology, **8**, 1, 20**18**.
8. SHAHREZAEI M., HABIBZADEH S., BABALUO A.A., HOSSEINKHANI H., HAGHIGHI M., HASANZADEH A., TAHMASEBPOUR R. Study of synthesis parameters and photocatalytic activity of TiO_2 nanostructures. Journal of Experimental Nanoscience, **12** (1), 45, **2017**.
9. KUMAR S.G., RAO K.S.R.K. Zinc oxide based photocatalysis: tailoring surfacebulk structure and related interfacial charge carrier dynamics for better environmental applications. RSC Advances, **5**, 3306, **2015**.
10. DI MAURO A., FRAGALA M.E., PRIVITERA V., IMPELLIZZERI G. ZnO for application in photocatalysis: From thin films to nanostructures. Materials Science in Semiconductor Processing, **69**, 44, **2017**.
11. LEE K.M., LAI C.W., NGAI K.S., JUAN J.C. Recent developments of zinc oxide based photocatalyst in water treatment technology: A review. Water Research, **88**, 428, **2016**.
12. ONG C.B., NG L.Y., MOHAMMAD A.W. A review of ZnO nanoparticles as solar photocatalysts: Synthesis, mechanisms and applications. Renewable and Sustainable Energy Reviews, **81**, 536, **2018**.
13. SAMADI M., ZIRAK M., NASERI A., KHORASHADIZADE E., MOSHFEGH A.Z. Recent progress on doped ZnO nanostructures for visible-light photocatalysis. Thin Solid Films, **605**, 1, **2016**.

14. MOHAMMAD MEHDI BANESHI, SAEEDEH JAHANBIN, ALI MOUSAVIZADEH, SEYED ABDOLMOHAMMAD SADAT, ALIREZA RAYEGAN-SHIRAZI, HAMED BIGLARI Gentamicin Removal by Photocatalytic Process from Aqueous Solution. Polish Journal of Environmental Studies, **27** (4), 1433, **2018**.
15. SINGH R., BARMAN P.B, SHARMA D. Synthesis, structural and optical properties of Ag doped ZnO nanoparticles with enhanced photocatalytic properties by photodegradation of organic dyes. Journal of Materials Science, Journal of Materials Science: Materials in Electronics, **28**, 5705, **2017**.
16. PRADEEV R.K., SADAIYANDI K., KENNEDY A., SAGADEVAN S., CHOWDHURY Z.Z., JOHAN M.R.B., AZIZ F.A., RAFIQUE R.F., THAMIZ S.R., RATHINA B.R. Influence of Mg Doping on ZnO Nanoparticles for Enhanced Photocatalytic Evaluation and Antibacterial Analysis. Nanoscale Research Letters, **13** (1), 229, **2018**.
17. HABBA Y.G., CAPOCHICHI-GNAMBODOE M., LEPRINE-WANG Y. Enhanced Photocatalytic Activity of Iron-Doped ZnO Nanowires for Water Purification. Applied Science, **7**, 1185, **2017**.
18. LAVAND A.B., MALGHE Y.S. Synthesis, characterization and visible light photocatalytic activity of carbon and iron modified ZnO. Journal of King Saud University – Science, **30**, 65, **2018**.
19. SUN S., CHANG X., LI X., LI Z. Synthesis of N-doped ZnO nanoparticles with improved photocatalytical activity. Ceramics International, **39** (5), 5197, **2013**.
20. SUDRAJAT H., BABEL S. A novel visible light active N-doped ZnO for photocatalyticdegradation of dyes. Journal of Water Process Engineering, **16**, 309, **2017**.
21. LAVAND A.B., MALGHE Y.S. Synthesis, characterization and visible light photocatalytic activity of nitrogen-doped zinc oxide nanospheres, Journal of Asian Ceramic Societies, **3**, 305, **2015**.
22. VERMA N., YADAV S., MARI B., MITTAL A., JINDAL J. Synthesis and Charcterization of Coupled ZnO/SnO_2 Photocatalysts and Their Activity towards Degradation of Cibacron Red Dye. Transactions of the Indian Ceramic Society, **77** (1), 1, **2018**.
23. CHANG Y-C. Complex ZnO/ZnS nanocable and nanotube arrays with high performance photocatalytic activity. Journal of Alloys and Compounds, **664**, 538, **2016**.
24. DING M., YANG H., YAN T., WANG C., DENG W., ZHANG S., HUANG J., SHAO M., XU X. Fabrication of Hierarchical ZnO@NiO Core–Shell Heterostructures for Improved Photocatalytic Performance. Nanoscale Research Letters, **13**, 260, **2018**.
25. KUNDU P., DESPANDE P.A, MADRAS G., RAVISHANKAR N. Nanoscale ZnO/CdS heterostructures with engineered interfaces for high photocatalytic activity under solar radiation. Journal of Materials Chemistry, **21**, 4209, **2011**.
26. REDDY C.V., BABU B., SHIM J. Synthesis, optical properties and efficient photocatalytic activity of CdO/ZnO hybrid nanocomposite. Journal of Physics and Chemistry of Solids, **112**, 20, **2018**.
27. CHEN Q., HOU H., ZHANG D., Hu S., MIN T., LIU B., YANG C., PU W., HU J., YANG J. Enhanced visible-light driven photocatalytic activity of hybrid ZnO/g-C_3N_4 by high performance ball milling. Journal of Photochemistry and Photobiology A: Chemistry, **350**, 1, **2018**.
28. YUAN X., ZHOU C., JIANG Q., TANG Q., MU Y., DU A. Facile Synthesis of g-C_3N_4 Nanosheets/ZnO Nanocomposites with Enhanced Photocatalytic Activity in Reduction of Aqueous Chromium (VI) under Visible Light. Nanomaterials, **6** (9), 173, **2016**.
29. LIU C., LI C., FU X., RAZIQ F., QU Y., JING L. Synthesis of silicate-bridged ZnO/g-C_3N_4 nanocomposites as efficient photocatalysts and its mechanism. *RSC Advances*, **5**, 37275, **2015**.
30. LIU P., GUO Y., XU Q., WANG F., LI Y., SHAO K. Enhanced photocatalytic performance of ZnO/multi-walled carbon nanotube nanocomposites for dye degradation. Ceramics International, **40**, 5629, **2014**.
31. MU J., SHAO C., GUO Z., ZHANG Z., ZHANG M., ZHANG P., CHEN B., LIU Y. High Photocatalytic Activity of ZnO-Carbon Nanofiber Heteroarchitectures. ACS Applied Materials & Interfaces, **3**, 590, **2011**.
32. ZHANG K., OH W-C. Effect of Heat-Treated Temperature on Surface Crystal Structure and Catalytic Activity of ACF/ZnO Composite under Ultraviolet Irradiation and Ultrasonication. Journal of Korean Ceramic Society, **47** (2), 136, **2010**.
33. LI Y., ZHANG B.-P., ZHAO J.-X., GE Z.-H., ZHAO X.-K., ZOU L. ZnO/carbon quantum dots heterostructure with enhanced photocatalytic properties. Applied Surface Science, **279**, 367, **2013**.
34. FENG C., DENG X-Y., Ni X-X., Li W-B. Fabrication of Carbon Dots Modified Porous ZnO Nanorods with Enhanced Photocatalytic Activity. Acta Physico Chimica Sinica, **31** (12), 2349, **2015**.
35. BOZETINE H., WANG Q., BARRAS A., LI M., HADJERSI T., SZUNERITS S., BOUKHERROUB R. Green Chemistry Approach for the Synthesis Of ZnO-Carbon Dots Nanocomposites With Good Photocatalytic Properties Under Visible Light. Journal of Colloid and Interface Science, **465**, 286, **2015**.
36. YU H., ZHANG H., HUANG H., LIU Y., LI H., MINGA H., KANG Z. ZnO/carbon quantum dots nanocomposites: one-step fabrication and superior photocatalytic ability for toxic gas degradation under visible light at room temperature. New Journal of Chemistry, **36**, 1031, **2012**.
37. ZHANG Z., ZHENG T., LI X., XU J., ZENG H. Progress of Carbon Quantum Dots in Photocatalysis Applications. Particle and Particle Systems Characterization, **33** (8), 457, **2016**.
38. YANG P., ZHAO J., WANG J., CUI H., LIA L., ZHU Z. Pure carbon nanodots for excellent photocatalytic hydrogen generation. RSC Advances, **5**, 21332, **2015**.
39. LI H, LIU R., LIAN S., LIU Y., HUANG H., KANG Z. Near-infrared light controlled photocatalytic activity of carbon quantum dots for highly selective oxidation reaction. Nanoscale, **5**, 3289, **2013**.
40. CHU K-W., LEE S.L., CHANG C-J., LIU L. Recent Progress of Carbon Dot Precursors and Photocatalysis Applications. Polymers, **11**, 689, **2019**.
41. WANG H-X., XIAO J., YANG Z., TANG H., ZHU Z-T., ZHAO M., LIU Y., ZANG C., ZHANG H-L. Rational design of nitrogen and sulfur co-doped carbon dots for efficient photoelectrical conversion applications. Journal of Material Chemistry A, **3**, 11287, **2015**
42. LI B.J., CAO H.Q. ZnO@graphene composite with enhanced performance for the removal of dye from water. Journal of Materials Chemistry, **21**, 3346, **2011**.